Advanced Composite Materials
Publication details, including instructions for authors and subscription information:
http://www.tandfonline.com/loi/tacm20

Estimation of five elastic stiffness coefficients of unidirectional glass fiber reinforced plastic by laser generated ultrasonic

Masayuki Iwasawa , Yoshihiro Mizutani , Hideo Nishino , Mikio Takemoto & Kanji Ono

Version of record first published: 02 Apr 2012.

To cite this article: Masayuki Iwasawa , Yoshihiro Mizutani , Hideo Nishino , Mikio Takemoto & Kanji Ono (2002): Estimation of five elastic stiffness coefficients of unidirectional glass fiber reinforced plastic by laser generated ultrasonic , Advanced Composite Materials, 11:2, 121-135

To link to this article: http://dx.doi.org/10.1163/156855102760410324

Adv. Composite Mater., Vol. 11, No. 2, pp. 121–135 (2002)

Also available online - www.vsppub.com

Estimation of five elastic stiffness coefficients of unidirectional glass fiber reinforced plastic by laser generated ultrasonic

MASAYUKI IWASAWA, YOSHIHIRO MIZUTANI, HIDEO NISHINO, MIKIO TAKEMOTO and KANJI ONO

Faculty of Science and Engineering, Aoyama Gakuin University, 6-16-1, Chitosedai, Setagaya, Tokyo 157-8572, Japan

Received 27 November 2000; accepted 20 February 2001

Abstract—Five elastic stiffness coefficients of UD-GFRP were estimated by using a laser iso-angular scanning method. Four stiffness coefficients C_{33}, C_{11}, C_{66} and C_{44} (direction 3 being the fiber direction) were first accurately determined by using phase velocities of longitudinal and shear waves in the fiber and fiber-normal directions. The stiffness C_{13} was estimated by iteration so that the slowness curve of quasi-shear waves computed to an assumed C_{13} best matches the measured one. The estimated stiffness coefficients agreed quite well with those estimated by the through-transmission method in water.

Keywords: UD-GFRP; laser iso-angular scanning method; quasi-shear wave; elastic stiffness coefficients; through transmission method in water.

1. INTRODUCTION

Accurate estimation of elastic stiffness coefficients of an anisotropic medium is important for integrity and damage inspection by ultrasonic and acoustic emission (AE). Extensive researches on the elastic stiffness estimation have been conducted so far. Some researchers utilized the orientation dependency of surface acoustic wave (SAW) velocities, and some that of bulk waves. The procedure for determining (recovering) the stiffness coefficients from the measured phase velocities of bulk waves has been addressed in detail by Every [1]. It is based on the Christoffel equation [2], a relation between the phase velocity and stiffness coefficients. However, the wave energy is propagated with group velocity and, in general, the phase velocity is different from the group velocity both in direction and magnitude.

Recently a point-transmitting and a point receiving system (a PT/PR system) was demonstrated to be a convenient method for measuring group velocities [3, 4]. Chai and Wu [5] estimated the elastic stiffness coefficients of a unidirectional glass fiber reinforced plastic (UD-GFRP) using the SAW group velocities, measured by a focused laser beam and a small aperture transducer located on the surface of medium. Castagnede *et al.* [6] generated bulk waves by a point-focused laser and received by a miniature piezoelectric transducer of 1.3 mm aperture or a miniature capacitive transducer of 3 mm diameter. This method, called iso-angular scanning (abbreviated as IAS hereafter), measures the group velocity of longitudinal (L-), shear (S-) and quasi-shear (QS-) waves in a symmetric plane by scanning the receiver along the fiber direction. As the bulk waves are generated and measured on the opposite surfaces of GFRP plate, the IAS method needs only one plate-shaped specimen, but requires an optimized inverse scheme of the group velocity anisotropy or slowness curve of three bulk mode waves. Inverse processing of group velocity anisotropy tends to produce a large error and result in wrong properties due to falling in local minimums during inverse processing. Due to finite aperture and waveform distortion by couplant, and also due to a limited specimen size, accurate determination of the arrival times of S- and QS-waves appears to be difficult. We once attempted to monitor the QS-waves by the IAS method; however, we could not monitor them due to many reflected wave peaks.

Park and Calder [7] utilized the phase velocity anisotropy of Rayleigh waves of graphite/epoxy composites. They excited the Rayleigh waves by a line-focused pulse YAG laser 15 mm long and monitored by a dual pinducer with 2.4 mm outer diameter. This system enabled a measurement of in-plane phase velocity anisotropy of the Rayleigh wave. The contact problem of a pinducer remains, but it can be minimized by utilizing a laser interferometer. Rose and Pilarski [8] recovered elastic stiffness coefficients of UD- and cross-ply CFRP by numerical analysis of the SAW velocities in the off-axis directions. Combined utilization of bulk, surface and subsurface waves are recommended by them. We estimated five stiffness coefficients of UD-CFRP, utilizing both the phase velocities of the Rayleigh wave and SSCW (surface skimming compressive wave) [9]. A point laser SAW system, consisting of a line-focused Nd-YAG laser and a heterodyne-type laser interferometer with an argon probe laser enabled us to determine the phase velocities of SAW. The laser interferometer measured the SAW on the mirror-surface CFRP; however, we could not measure the transmitted S- and/or QS-waves through rough surface GFRP. An advanced interferometer with a high power probe laser, applicable to rough surface, was needed for GFRPs with sprayed coating.

Other ultrasonic techniques employed so far are the immersed through-transmission [10] and double through-transmission method [11, 12]. Here, the arrival times of L-, S- and QS-waves transmitted through a medium set in water were measured as a function of the sample's rotation angle and receiver position. This technique requires a sophisticated computer controlled swivel table and a linear slider for

the receiver. A relatively thick medium is preferred for this method. Ultrasonic microscopy has recently been used, but this is limited to small media.

In this research, we aimed to measure the five stiffness coefficients of UD-GFRP with 60 mass% fiber content, using the laser IAS (LIAS) method. Here, we used a point focused pulse YAG laser (breakdown of silicone painted on the surface) as a transmitter and a heterodyne-type laser interferometer with a diode-pumped YAG probe laser as a receiver. The latter first enabled us to measure the S- and QS-waves embedded in many reflected waves. We measured group velocity anisotropy of L-, S- and QS-waves using four types of sample with different fiber orientations. We propose a simplified inversion scheme which can accurately determine the five stiffness coefficients and avoid the ill-condition (fall in local minimum) during inverse processing.

We first determined four stiffness coefficients: C_{11}, C_{33}, C_{44} and C_{66} (direction 3 being the fiber direction). Here, C_{33} and C_{11} were explicitly determined from the phase velocities of L-waves in the fiber and fiber-normal directions, respectively, C_{44} and C_{66} from the phase velocities of S-waves in fiber and fiber-normal directions. The coefficient C_{13} was determined by iteration so that the group velocity anisotropy calculated to an assumed C_{13} and predetermined four coefficients best matches the measured group velocity anisotropy (slowness curve) of QS-waves.

Next, we examined the accuracy of stiffness coefficients recovered, by comparing with those estimated by the immersed through-transmission method. We used two types of sample for this method, and estimated four stiffness coefficients (C_{11}, C_{13}, C_{33} and C_{44}). We propose a new method to determine two coefficients (C_{13} and C_{44}) correctly. The four coefficients determined by the LIAS method agreed well with those determined by the through-transmission method. The coefficient C_{66}, however, could not be determined by the through-transmission method.

2. TEST SPECIMEN AND EXPERIMENTAL METHOD

A UD-GFRP plate, 10.1 mm thick, was prepared by a filament winding method of E-glass fiber rovings (6400 fibers of 15 μm diameter single fiber) and vinylester resin. Fiber content of the specimen was measured as 60 mass% and density as 1844 kg/m^3. UD-GFRP is a transverse isotropic material with a symmetric axis in the X_3 direction. Five elastic stiffness coefficients are formulated in a matrix format (1):

$$\begin{bmatrix} C_{11} & C_{12} & C_{13} & 0 & 0 & 0 \\ C_{12} & C_{11} & C_{13} & 0 & 0 & 0 \\ C_{13} & C_{13} & C_{33} & 0 & 0 & 0 \\ 0 & 0 & 0 & C_{44} & 0 & 0 \\ 0 & 0 & 0 & 0 & C_{44} & 0 \\ 0 & 0 & 0 & 0 & 0 & C_{66} \end{bmatrix}. \tag{1}$$

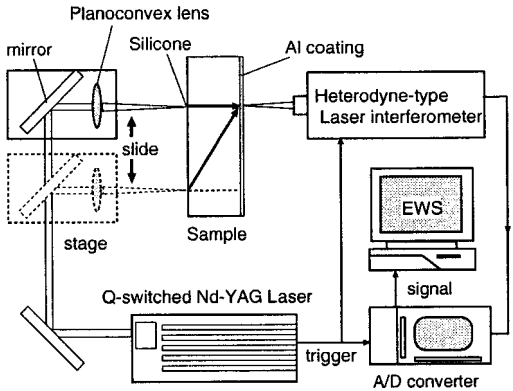

Figure 1. Laser iso-angular scanning method (LIAS).

Here $C_{12} = C_{11} - 2C_{66}$. We define θ as the wave energy propagation direction with respect to the fiber axis: $\theta = 0^\circ$ designates the fiber direction and $\theta = 90^\circ$ indicates the normal to the fiber axis.

Figure 1 shows the LIAS method. A Q-switched pulse YAG laser of half-height duration 50 ns was irradiated onto the specimen surface painted with silicone. Bulk waves, excited by a breakdown of silicone, were measured at the aluminum-coated opposite surface by a heterodyne-type laser interferometer with a diode-pumped YAG probe laser. Output of the laser interferometer, triggered by the incident YAG laser, was digitized by a fast A/D converter at sampling interval 4 ns with 4096 points. Digital data were fed into a work station. Wave propagation direction was changed by moving the stage with both a mirror and plano-convex lens for incident YAG laser. It was controlled by a computer controlled stepping motor at 2 μm spatial resolution. Four types of sample with different fiber orientations were used. These are shown in Fig. 2. Here, the angle ϕ denotes the angle of transmitter-receiver direction relative to the surface normal of samples. Types 3 and 4 are the same sample, but just inverted with respect to each other.

Figure 3 shows the immersed-through transmission method. We generated, by using a high damping compression-type PZT transmitter (Panametric, 10 MHz resonant, 10 mm aperture diameter), a longitudinal wave into water (25°C) and monitored the transmitted waves by a pinducer of 2.4 mm diameter, located at 41.7 mm from the transmitter. The pinducer enables us to determine the receiver's positions accurately. It was scanned by a computer controlled linear stage at 0.5 mm steps from the original position (s = 0 mm) to receive the wave with the largest amplitude. The sample was rotated through an angle ψ by a swivel table in 2° steps. The output of the pinducer was digitized at 10 ns with 4096 points. Two types of sample, Types 1 and 2 in Fig. 2, were used to determine the phase velocity of L- and QS-waves.

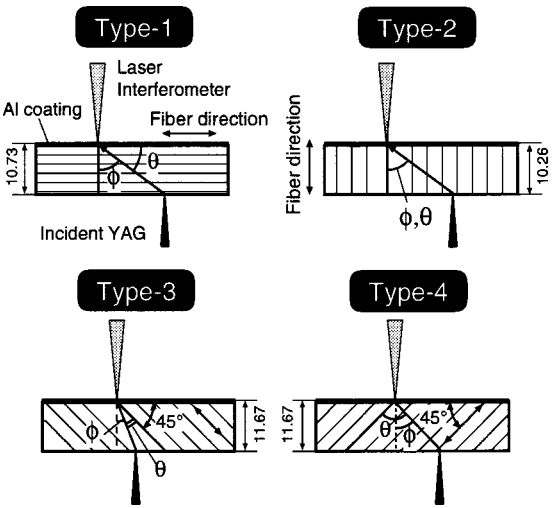

Figure 2. Four types of sample with different fiber orientations.

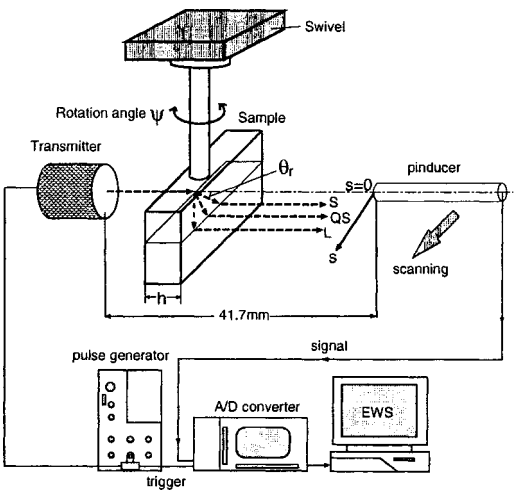

Figure 3. Immersed through-transmission method with typical wave propagation paths.

The phase velocities V_p of L- and QS-waves were calculated by equation (2).

$$V_p(\varphi) = \left[\frac{1}{V_w^2} - \frac{2\Delta t \cos\theta_r}{hV_w} + \frac{(\Delta t)^2}{h^2}\right]^{-1/2},$$
$$\Delta t = t - t_g, \tag{2}$$
$$\varphi = \arcsin\left[\frac{V_p(\theta_r)\sin\theta_r}{V_w}\right].$$

Here ,V_w designates the velocity of longitudinal wave in water, and is measured as 1495 m/s; h refers to the sample thickness (10.20 mm for Type 1 and 24.69 mm for Type 2). Δt is the time difference between the first wave arrival through and without sample. θ_r is given in equation (2).

3. RESULTS

3.1. Elastic stiffness coefficients determined by laser iso-angular scanning (LIAS) method

Figure 4 represents waveforms obtained for Type 1 and Type 2 samples. Symbols L, QS and S near the waves designate the arrival time of longitudinal, quasi-shear and shear waves. Symbols a, b and c are the predicted arrival time of reflected waves by three paths shown in Fig. 5. Here, the arrival times are calculated using the recovered stiffness coefficients shown in Table 1. Symbol a means the reflection of L-wave in thin Type 2 sample. Symbol b indicates the reflection at upper surface for Type 1 and Type 2 samples. Symbol c denotes the side-edge reflection observed

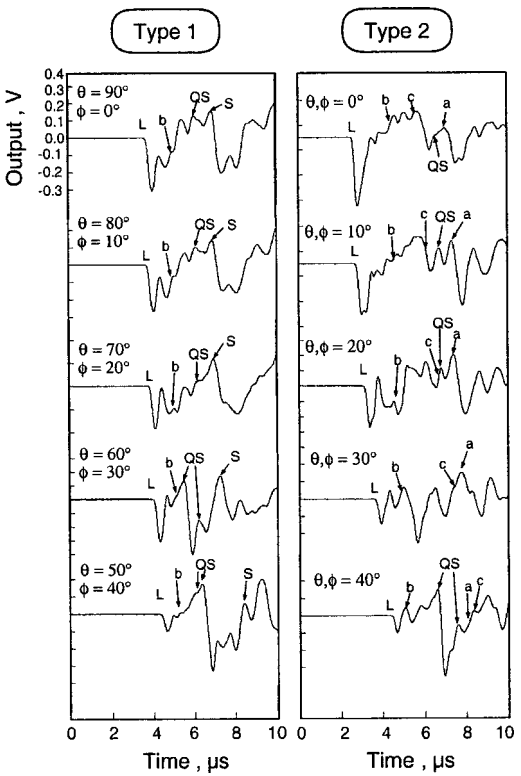

Figure 4. Waveform obtained by LIAS method for Type 1 and Type 2 samples.

for Type 2. Other peaks without symbols appear to be due to more complicated reflection paths.

Characteristic features of waves in Fig. 4 are: (1) peak amplitudes of the first arriving L-wave are larger near $\theta = 0^\circ$ and 90°, while (2) peak amplitudes of QS-waves are larger in the range of $35^\circ < \theta < 55^\circ$, and (3) two QS-peaks are observed at $\theta = 35^\circ, 40^\circ, 50^\circ, 55^\circ$ and 60°.

Traveling time of the L-wave was determined by zero-crossing time, but those of the QS- and S-waves were governed by peak times. Figure 6 compares waveforms

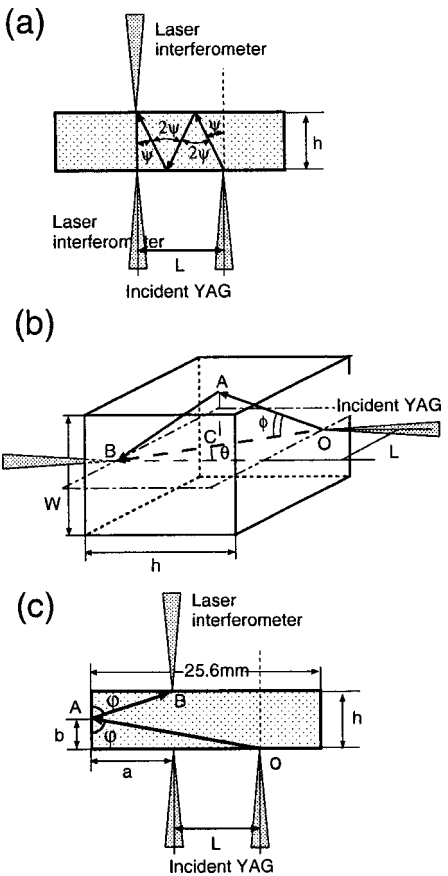

Figure 5. Predicted paths of reflected waves and propagation length; p.l and time; t.

Table 1.
Elastic stiffness coefficients of UD-GFRP estimated by TT method (GPa)

C_{33}	C_{11}	C_{13}	C_{44}	C_{66}
46.6	18.8	7.8	6.0	—

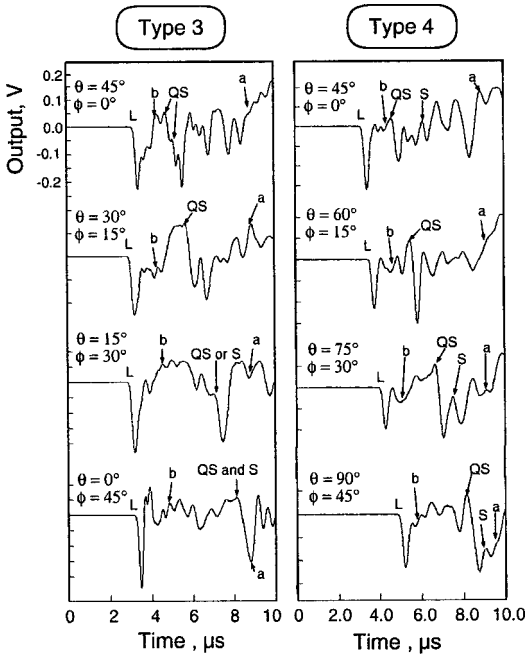

Figure 6. Waveform obtained by LIAS method for Type 3 and Type 4 samples.

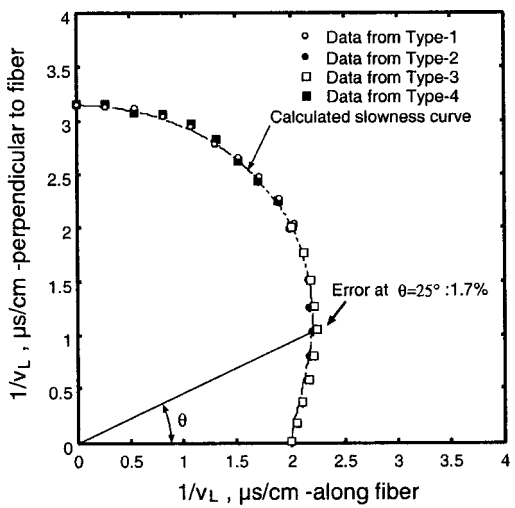

Figure 7. Orientation dependency of L-wave group velocity.

monitored for Type 3 and Type 4 samples. For the Type 4 sample, we can monitor clear QS-waves at $\theta > 60^\circ$. Orientation dependency (slowness curve) of the L-wave group velocities is shown in Fig. 7. Data from all types of sample agrees well within the maximum error of 1.7% at $\theta = 25^\circ$. Using the L-wave phase velocities at $\theta = 0^\circ$

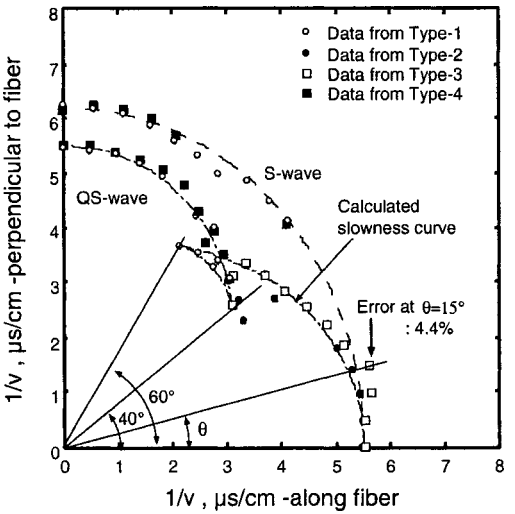

Figure 8. Orientation dependency of QS- and S-wave group velocity.

(5020 m/s) and 90° (3179 m/s), we determined C_{33} and C_{11} as 46.5 and 18.6 GPa, respectively. The solid line designates the slowness curve calculated from the finally determined five stiffness coefficients (Table 1). A good coincidence demonstrates the accuracy of the estimated stiffness coefficients.

Figure 8 represents the slowness curve of S- and QS-waves. Maximum deviation of the S-wave velocity from the calculated slowness curve was 4.4% at $\theta = 15°$. Using the phase velocities of S-waves at $\theta = 0°$ (1821 m/s) and 90° (1611 m/s), C_{44} and C_{66} are determined as 6.1 GPa and 4.8 GPa, respectively.

The slowness curve of QS-velocity shows two cusps at around $\theta = 40°$ and 60°. We determined C_{13} as follows. Orientation dependence of phase velocities of QS-waves are given by equation (3):

$$\frac{1}{V_{QS}} = \sqrt{\frac{2\rho}{(a-b)}},$$
$$a \equiv C_{11}\sin^2\theta + C_{33}\cos^2\theta + C_{44}, \tag{3}$$
$$b \equiv [\{(C_{11} - C_{44})\sin^2\theta + (C_{44} - C_{33})\cos^2\theta\}^2 + (C_{13} + C_{44})^2 \sin^2 2\theta]^{1/2}.$$

As four coefficients, C_{33}, C_{11}, C_{44} and C_{66}, have been determined, we first calculated the orientation dependency of QS-wave phase velocities to an assumed C_{13}, and then converted them to group velocities. Figure 9 shows curve fitting to find the most suitable C_{13}. Among three C_{13} values assumed, a curve computed to $C_{13} = 7.8$ GPa best matches the experimental data in the range $40° < \theta < 60°$. The slowness curve, calculated by using $C_{13} = 7.8$ GPa (Fig. 8), best fits the experimental data. Estimation accuracy of C_{13} is generally poor. It might be better to

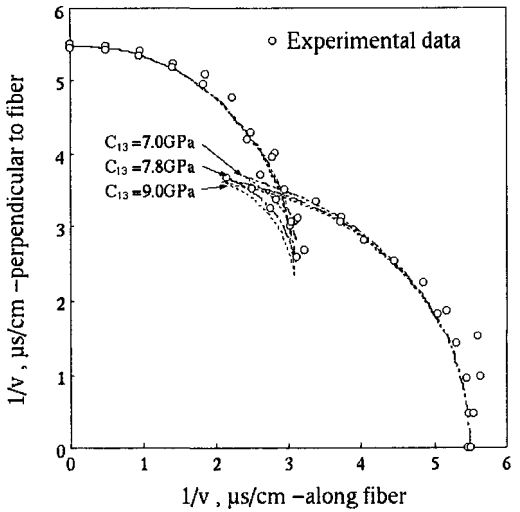

Figure 9. Orientation dependence of QS-wave group velocity anisotropy.

Table 2.
Elastic stiffness coefficients of UD-GFRP estimated by LIAS method (GPa)

C_{33}	C_{11}	C_{13}	C_{44}	C_{66}
46.5	18.6	7.8	6.1	4.8

say that C_{13} appears to be around 7.8 GPa. Five stiffness coefficients are shown in Table 2. An anisotropy factor $\eta(= 2C_{44}/(C_{11} - C22))$ is calculated as 0.25.

Castagnede *et al.* [6] reported an intersection of S- and QS-slowness curves in the anisotropic plane (1–3 plane) of UD-GRRP. This appears to be due to erroneous recovery of stiffness coefficients, by using the measured group velocities as the phase velocities. No intersection of S- and QS-slowness curves is reported for CFRP by Rose and Pilarski [8].

3.2. Elastic stiffness coefficients determined by the through-transmission method

Figure 10 shows an example of waves monitored for Type 1 sample at $\psi = 6^\circ$ (the top). This was obtained by the pinducer at position $s = 2.5$ mm as shown in the bottom figure. Phase velocity of P-wave was determined using the time difference $(t - t_w)$ between two peak times of P-waves measured through a sample t and without a sample t_w, and also $\theta = 76.9^\circ$, $\theta_r = 13.1^\circ$. Due to the complicated waveform, we could not determine the arrival time of the S-wave, possibly arriving at around 27 μs. Shown in Fig. 11 are waves monitored for Type 1 sample for $34.6^\circ < \theta < 90^\circ$. The L-wave amplitude decreases with decreasing θ (top to bottom in the left figure), and diminishes at around $\psi = 18^\circ$, while we observe

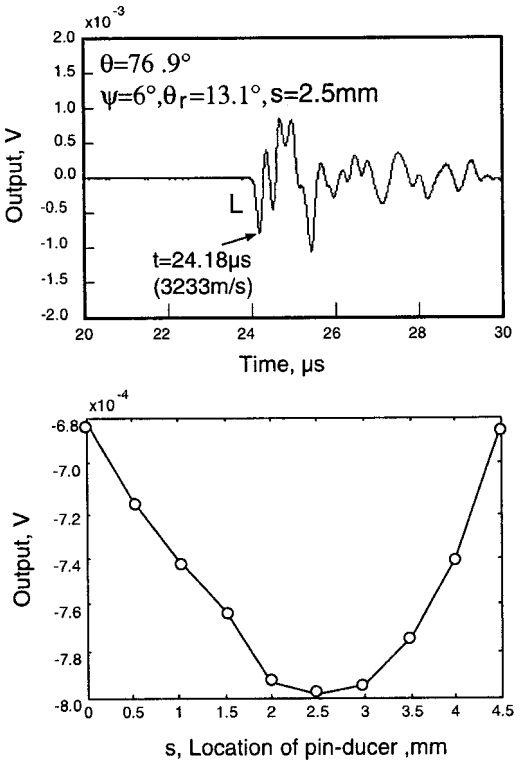

Figure 10. Wave monitored by through-transmission method for Type 1 sample at $\Psi = 6^\circ$ (top) and change of the first L-peak (bottom) with s.

clear QS-waves at θ from 34.6° to 58° (in the right figure). Figure 12 shows the waves monitored for Type 2 sample.

The slowness curve of L- and QS-waves are represented in Fig. 13. C_{11} and C_{33} are determined from L-wave phase velocities at $\theta = 0^\circ$ and 90° as 46.6 and 18.8 GPa, respectively. Solid lines are the computed slowness curve of the phase velocities using the stiffness coefficients in Table 1.

In this method, we estimated C_{13} and C_{44} from QS-wave velocities by the following scheme. We first examined the effect of C_{13} and C_{44} on the velocity anisotropy. Figure 14a shows QS-phase velocity distributions to three C_{13} values and Fig. 14b those to three C_{44} values. It is noted that the maximum velocity of QS-wave is significantly affected by C_{13}, while it is not affected by C_{44}. Contrary to this, the width of distribution changed depending on the C_{44} as shown in Fig. 14b. Thus we first determined the C_{13} so that the maximum velocity fitted the measured value by using appropriate C_{44}. We estimated C_{13} as 7.8 GPa. Then C_{44} was determined as 6 GPa. This method enabled us to determine C_{13} and C_{44} from limited QS data. However we could not determine C_{66}, since we could not measure the velocity of the S-wave in the fiber normal direction by any method. We attempted to measure the

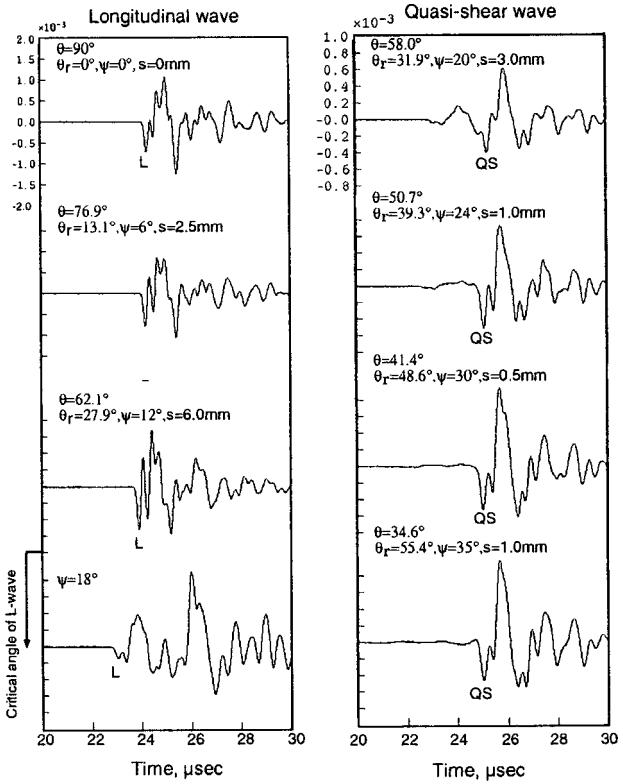

Figure 11. Waves monitored for Type 1 sample.

S-wave velocity by a counter contact method of two S-wave transducers; however, we could not determine the arrival time due to a long trailing P-wave.

A good agreement of the four stiffness coefficients in Tables 1 and 2 demonstrates the usefulness of the proposed LIAS method using four types of sample.

4. CONCLUSIONS

We have recovered five elastic stiffness coefficients of a unidirectional glass fiber reinforced plastic (direction 3 being the fiber direction), utilizing a new inverse method of group velocity anisotropy of bulk mode waves measured by the laser iso-angular scanning method. The proposed method needs four types of samples with different fiber direction; however, this enables an accurate determination of five stiffness coefficients. This method can reduce the uncertainty often observed during conventional inverse processing of slowness curve. The estimated stiffness coefficients were compared with that estimated by the through-transmission method.

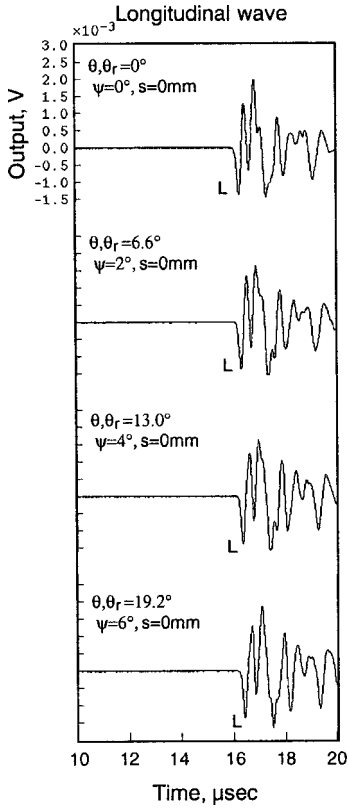

Figure 12. Waves monitored for Type 2 sample.

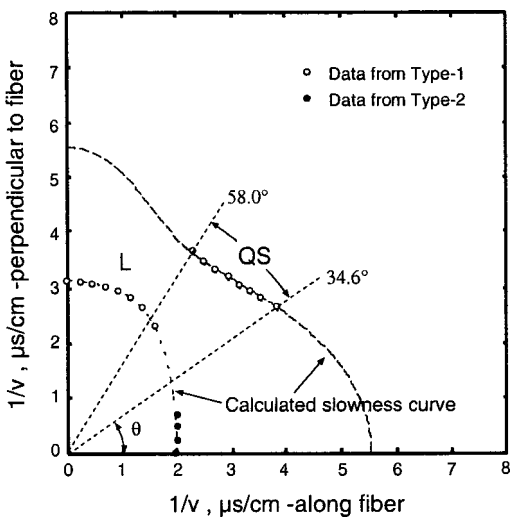

Figure 13. Orientation dependence of the phase velocity of L- and QS-waves.

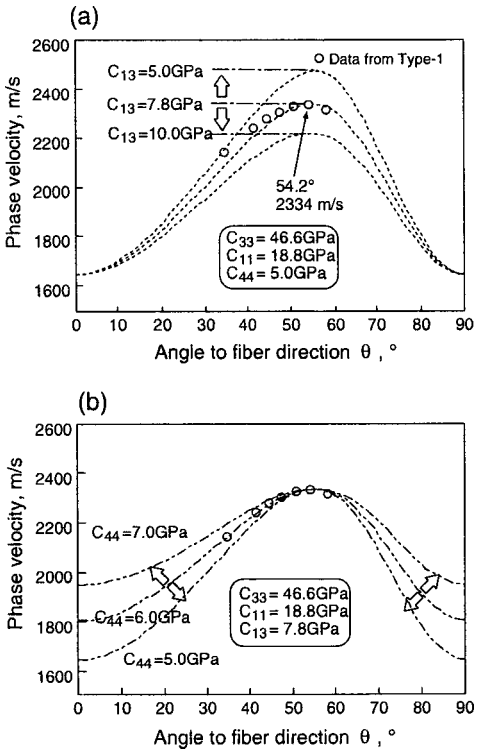

Figure 14. QS-phase velocity distribution as a function of C_{13} (a) and C_{44} (b).

Results are summarized below:

1) A laser iso-angular scanning (LIAS) method, consisting of a point pulse YAG laser transmitter and a hetero-dyne type laser interferometer with a high power YAG probe laser, enabled us to measure the group velocities of longitudinal (L-), shear (S-) and quasi-shear (QS-) waves of UD-GFRP with rough surface.
2) We used four types of sample with different fiber orientations, and measured the phase velocities of L- and S-waves in the fiber and fiber normal directions. C_{33} and C_{11} were accurately determined from the L-wave phase velocities in the fiber and fiber normal directions, respectively. We also determined C_{44} and C_{66} from the phase velocities of S-waves in the fiber and fiber normal directions, respectively.
3) The coefficient C_{13} was determined by iteration so that the slowness curve of QS-wave group velocities, calculated to an assumed C_{13} and predetermined four stiffness coefficients, best matches that of the measured curve.
4) We proposed a new method to recover the four stiffness coefficients, C_{33}, C_{11}, C_{13} and C_{44}, from the through-transmission data obtained from two types of sample with fibers in parallel and perpendicular to the sample surface. C_{33} and C_{11} were determined from L-wave phase velocities in fiber and fiber

normal directions. C_{13} and C_{44} are recovered so that the maximum velocity and velocity distribution of computed QS-wave velocity anisotropy matches the measured data. The coefficient C_{66} could not be determined since the S-wave velocity in the fiber normal direction could not be measured by any method.

5) Four stiffness coefficients estimated from the through-transmission method agreed quite well (within the maximum error of 1.7%) with that estimated by the LIAS method.

REFERENCES

1. A. G. Every, General closed form expression of acoustic wave in elastically anisotropic solids, *Phys. Rev.* **B22**, 1746–1760 (1980).
2. C. B. Scurby, Some applications of laser ultrasound, *Ultrasonics* **27**, 195–209 (1989).
3. K. Y. Kim, W. Sachse and A. G. Every, On the determination of sound speed in cubic crystals and isotropic media using a broad band ultrasonic point-source/point-receiver method, *J. Acoustic Soc. Amer.* **93** (3), 1393–1406 (1993).
4. A. G. Every and W. Sachse, Determination of the elastic constants of anisotropic solid from acoustic wave group measurement, *Phys. Rev.* **B42**, 8196–8205 (1990).
5. J.-F. Chai and T.-T. Wu, Determinations of anisotropic elastic constants using laser-generated surface waves, *J. Acoustic Soc. Amer.* **95** (6), 3233–3241 (1994).
6. B. Castagnede, K. Y. Kim and W. Sachse, Determination of the elastic constants of anisotropic materials using laser-generated ultrasonic signals, *J. Appl. Phys.* **70** (1), 150–157 (1991).
7. H. Park and C. Calder, Laser generated Rayleigh waves in graphite/epoxy composites, *Experimental Mechanics*, pp. 148–154 (1994).
8. J. L. Rose and A. Pilarski, An ultrasonic NDE surface wave feature matrix technique for composite materials, in: *Wave Propagation In Structural Composites, ASME AMD-90,* A. K. Mal and T. C. T. Ting (Eds), pp. 117–131 (1988).
9. Y. Mizutani and M. Takemoto, A simplified elastic stiffness estimation of unidirectional carbon-carbon fiber-reinforced coupon using the in-plane velocity anisotropy of Lamb waves, *Jap. J. Applied Phys.* **37**, 3110–3115 (1998).
10. K. Balasubramaniam and S. C. Whitney, Ultrasonic through-transmission characterization of thick fiber-reinforced composites, *NDT and E Int.* **29** (4), 225–236 (1996).
11. S. I. Rohklin and W. Wang, Double through-transmission bulk wave method for ultrasonic phase velocity measurement and determination of elastic constants of composite materials, *J. Acoustic Soc. Amer.* **91**, 3303–3312 (1992).
12. K. Kawashima, I. Fuji, A. Yamamoto, Y. Shimiszu and A. Fukushima, Measurement of anisotropic elastic constants of sandwiched SiC/Ti composite by double transmission, critical angle and leaky surface wave technique, in: *Review of Progress in NDE*, Vol. 16, pp. 1663–1668 (1997).